RSC Advances

ROYAL SOCIETY OF CHEMISTRY

www.rsc.org/advances

RSC Advances

ARTICLE

Influence of phenolphthalein groups on the structure and properties of poly(arylene ether sulfone nitrile)s-based anion exchange membranes for fuel cells

Received 00th January 20xx,
Accepted 00th January 20xx

DOI: 10.1039/x0xx00000x

www.rsc.org/

Ao Nan Lai, Yi Zhi Zhuo, Chen Xiao Lin, Qiu Gen Zhang, Ai Mei Zhu, Mei Ling Ye and Qing Lin Liu*

Two series of novel poly(arylene ether sulfone nitrile)s (PESN) multiblock copolymers are synthesized to prepare anion exchange membranes (AEMs) for alkaline fuel cells. To study the effect of phenolphthalein groups on the structure and properties of the membranes, the ion groups facilitating the formation of ion clusters are selectively and densely located on the phenolphthalein-sulfone segments for one and on the bisphenol A-sulfone segments for the other. The morphology and structure of the membranes are observed by atomic force microscopy and small angle X-ray scattering. The phenolphthalein-containing type endows the AEMs with a much clearer and more-defined microphase-separated structure leading to the formation of much larger and more developed interconnected ion-transport channels. As a result, high hydroxide conductivity (in the range of 2.04–12.98 $\times 10^{-2}$ S cm^{-1} from 30 to 80 °C) and H_2/O_2 fuel cell performance (an open circuit voltage of 0.92 V and a maximum power density of 66.4 mW cm^{-2} at 60 °C) can be achieved. Furthermore, the phenolphthalein-containing AEMs also show higher water uptake and mechanical strength, lower swelling ratio, and higher thermal and alkaline stability than the phenolphthalein-free AEMs.

Introduction

Polymer electrolyte fuel cells (PEFCs) are one of the most promising power sources that have high energy density and efficiency, low noise, and low pollution.[1,2] Currently, perfluorosulfonic acid ion exchange membranes (such as Nafion) are preferentially used in the development of proton exchange membrane fuel cells (PEMFCs).[3,4] However, the serious matters including fuel crossover, the requirement of noble metal catalysts, conductivity loss at elevated temperature, and high cost of perfluorinated membranes impede the commercialization of PEMFCs. Recently, anion exchange membrane fuel cells (AEMFCs) have emerged as an alternative due to their several advantages over PEMFCs: (1) Higher pH provides faster fuel oxidation kinetics, (2) AEMFCs can operate with non-noble metal catalysts (such as Ni and Co), (3) the reverse electro-osmosis reduces the fuel crossover, and (4) the fuel is flexible (methanol, ethanol, ethylene glycol, etc.).[5-8] However, AEMFCs suffer from the insufficient ion conductivity or/and alkaline stability of the existing AEMs which limit their applications. Numerous researches indicate that the nanophase separation can create ion-conducting channels and facilitate the ion transport through membranes.[9-11] This provides an effective way to develop highly anion-conductive AEMs. To perform this strategy, several methods could be used, such as using block copolymers as the backbones of membranes,[12-15] introducing branched or pendant ion groups into the membrane matrices,[16-18] and controlling the position and density of ion groups.[19-21]

Copolymers containing phenolphthalein groups showed excellent mechanical properties, and high thermal and chemical stability.[22] For this reason, attempts have been made to the preparation of phenolphthalein-containing copolymers as ion conductive membranes in the last few years. Zhang et al. prepared phenolphthalein-based cardo poly(arylene ether sulfone)s PEMs and assumed that introducing phenolphthalein groups into the copolymer main chain could provide large free volume in which water could be stored and be beneficial for PEM applications.[23-25] Phenolphthalein-based AEMs were also synthesized by chloromethylation, quaternization and ion exchange on commercial phenolphthalein-based cardo PES and PEK polymers.[26-28] Recently, we synthesized a series of imidazolium group-bearing phenolphthalein-based poly(arylene ether sulfone nitrile)s multiblock copolymers as AEMs. The AEMs showed a well-defined hydrophilic/hydrophobic microphase-separated morphology to form interconnected ion-transport channels. The high ionic conductivity of the AEMs in the range of 3.85–14.67$\times 10^{-2}$ S cm^{-1} increased with increasing the hydrophilic block length and temperature. Moreover, the

Department of Chemical & Biochemical Engineering, College of Chemistry & Chemical Engineering, Xiamen University, Xiamen 361005, China. E-mail: qlliu@xmu.edu.cn

† Electronic Supplementary Information (ESI) available: ^{1}H NMR spectra of oligomer-PF, oligomer-IF, and oligomer-OH; ^{1}H NMR spectra of MPPESN and MPESN; ^{1}H NMR spectra of BrPPESN-2.87 and BrPESN-2.92; ^{1}H NMR spectra of BrPPESN-x prepared with various molar ratios of NBS to MPPESN; ^{1}H NMR spectra of ImPPESN-2.87 and ImPESN-2.92; FT-IR spectra of ImPPESN-2.87 before and after the alkaline stability test, and of ImPESN-2.92 before and after the alkaline stability test; ^{1}H NMR spectra of ImPPESN-2.87 before and after the alkaline stability test; ^{1}H NMR spectra of ImPESN-2.92 before and after the alkaline stability test. See DOI: 10.1039/x0xx00000x

AEMs also showed low swelling, good mechanical strength and thermal stability, and acceptable alkaline stability in a 2 M KOH solution at 60 °C for 600 h.[29] However, the structure-property relationship, especially the effect of the phenolphthalein group on the morphology and properties of the membrane, which is particularly important for the design of AEMs, is not clear.

In this study, two kinds of poly(arylene ether sulfone nitrile)s (PESN) multiblock copolymers were synthesized via block copolycondensation. The copolymers were subsequently brominated and imidazolium-functionalized to prepare AEMs. The difference between them is that the ion groups are selectively and densely located on the phenolphthalein-sulfone segments for one and on the bisphenol A-sulfone segments for the other. Their chemical structures were confirmed by FT-IR and ^{1}H NMR. The influence of the phenolphthalein group on the structure and properties of the membrane, such as water uptake, swelling ratio, hydroxide conductivity, mechanical and thermal properties, and alkaline stability, was investigated in detail. The effect of the density of imidazolium groups in the membrane matrix on the properties of the AEMs was also evaluated. The ImPESN-19-22 membrane reported in our previous work,[29] which has a similar density of imidazolium groups to the phenolphthalein-free AEMs prepared in this work, was used in this report (termed ImPPESN-2.87) to make a comparison.

Experimental

Materials

2,6-Difluorobenzonitrile (DFBN; 99%, Aladdin, China), bis(4-fluorophenyl) sulfone (FPS; 99%, TCI, Japan), bisphenol A (BHA; 97%, Sigma-Aldrich, St. Louis, MO), 4,4'-isopropylidenebis (2,6-dimethylphenol) (DMBHA; 98%, Sigma-Aldrich, St. Louis, MO), N-bromosuccinimide (NBS; 99%, Aladdin, China), and 1-methylimidazole (MIm; 99%, Aladdin, China) were used as received. The monomer 3,3-bis(4-hydroxyl-3,5-dimethylphenyl)-phenolphthalein (DMPPH) was prepared as previous described.[29] N,N-dimethylacetamide (DMAc; 99.8%, Aladdin, China) and toluene were purified by stirring over CaH_2 for 24 h, distilling under reduced pressure, and storing over 4 Å molecular sieves. Benzoyl peroxide (BPO; 99%, Sinopharm, China) was obtained from Tianjin Guangfu Fine Chemical Research Institute (China) and purified by recrystallizing from chloroform. All other chemicals were purchased from Shanghai Sinopharm Chemical Reagent Co., Ltd (China) and used as received.

Preparation of the imidazolium functionalized poly(arylene ether sulfone nitrile)s (ImPESN) AEMs

Synthesis of isopropylidene-containing fluorine-terminated telechelic oligomers (oligomer-IF) and hydroxyl-terminated telechelic oligomers (oligomer-OH)

Oligomer-IF was synthesized by the method reported in the literature.[29] A typical procedure for the synthesis of oligomer-IF is as follows. 2.8439 g (10 mmol) of DMBHA, 2.6696 g (10.5 mmol) of FPS, 3.4553 g (25 mmol) of K_2CO_3, 30 mL of DMAc and 15 mL of toluene were added to a 100 mL three-necked round-bottomed flask equipped with a magnetic stirrer and a Dean-Stark trap. Under a nitrogen atmosphere, the reaction mixture was heated at 140 °C for 4 h and subsequently raised to 165 °C for another 12 h. To ensure the end-capping, 50 mg of FPS was added at the end of the reaction. Afterwards, the resulting solution was cooled to room temperature (RT) and precipitated in 400 mL of an aqueous methanol solution (deionized (DI) water/methanol=1/1, v/v). The precipitate was magnetically stirred in the aqueous methanol solution at 80 °C for 5 h, filtered and purified with methanol in a Soxhlet extractor for another 12 h. After drying under vacuum at 60 °C for 48 h, we obtained oligomer-IF. The polymerization degree of oligomer-IF was m=17 from GPC.

Oligomer-OH was prepared as previous described.[29] The polymerization degree of oligomer-OH was n=22 from GPC.

Synthesis of multiblock tetramethyl poly(arylene ether sulfone nitrile)s (MPESN)

MPESN was synthesized by the method reported in the literature.[29] A typical procedure for the synthesis of the block copolymers MPESN is as follows (Scheme 1). An equimolar amount of oligomer-OH and oligomer-IF mixed with K_2CO_3 were charged into a 100 mL three-necked round-bottomed flask. DMAc was used as the solvent, and was toluene used as the azeotropic agent for water removal during the reaction. The mixture was stirred at 145 °C for 4 h under nitrogen and then slowly increased to 165 °C for another 20 h after removing the toluene. After the polymerization, the viscous copolymer solution was cooled to RT and precipitated in 400 mL of an aqueous methanol solution (DI water /methanol=1/1, v/v). Then the copolymer was magnetically stirred in the aqueous methanol solution at 80 °C for 5 h, filtered and purified with methanol in a Soxhlet extractor for another 12 h. After drying in a vacuum oven at 60 °C for 48 h, a white MPESN solid was obtained (yield: 89%).

Bromination of MPESN

The bromination reaction of the MPESN was carried out using NBS as the bromination agent and BPO as the initiator in a 1,1,2,2-tetrachloroethane (TCE) solution (Scheme 1). A typical procedure is as follows. 20 mL of TCE and 1.0 g of MPESN were introduced into a 100 mL three-necked round-bottomed flask and heated to 85 °C under stirring to make a homogeneous solution. Then 0.8046 g of NBS and 0.0547 g of BPO were added to the solution. The mixture was maintained at 85 °C for 5 h under nitrogen. Upon cooling to RT, the mixture was precipitated in 400 mL of a methanol solution. The precipitate was subsequently filtered, purified with methanol in a Soxhlet extractor for 12 h, and dried under vacuum at 60 °C for 48 h to yield a yellow product. The obtained copolymer is termed BrPESN-x, where Br denotes the bromination reaction and x is the degree of functionalization (DF), which is defined as the number of bromomethyl groups per copolymer repeating unit.

Synthesis of imidazolium functionalized poly(arylene ether sulfone nitrile)s (ImPESN) and membrane formation

ImPESN was prepared from the nucleophilic substitution

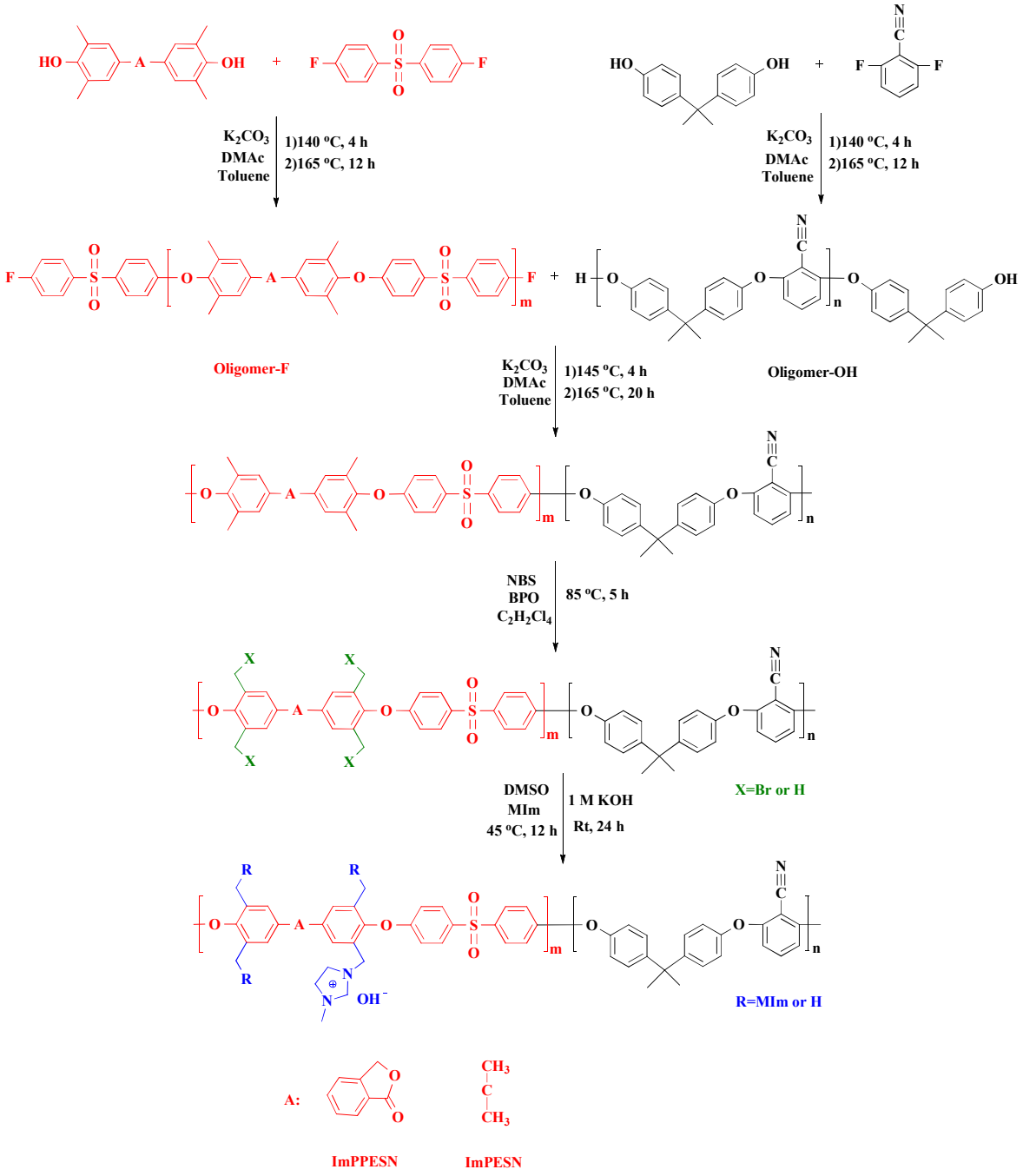

Scheme 1 Synthesis of poly(arylene ether sulfone nitrile)s based AEMs.

reaction between BrPESN and MIm (Scheme 1). A typical procedure was as follows. 1.0 g of BrPESN-2.92 was dissolved in 20 mL of dimethyl sulfoxide (DMSO) in a 50 mL round-bottomed flask and heated to 45 °C under stirring. After completely dissolved, 1.12 mL of MIm was introduced slowly. The solution was stirred at 45 °C for 12 h, and filtered using a 0.45 μm PTFE membrane. The filtered solution was cast directly onto a clean and dry glass plate and dried at 60 °C under vacuum for 48 h to obtain a transparent membrane. The membrane in salt form was converted to OH^- form by immersing in a 1 M KOH solution at RT for 24 h followed by keeping in DI water for 24 h before use. The obtained membrane is termed ImPESN-x, where Im denotes the imidazolium functionalization.

Fabrication of the imidazolium functionalized phenolphthalein-containing poly(arylene ether sulfone nitrile)s (ImPPESN) AEMs.

The multiblock tetramethyl phenolphthalein-containing poly(arylene ether sulfone nitrile)s (MPPESN) and imidazolium

functionalized phenolphthalein-containing poly(arylene ether sulfone nitrile)s (ImPPESN) were synthesized as previous described.[29] Besides, the BrPPESN-x with different DFs can be obtained by adjusting the molar ratio of NBS to MPPESN.

Characterization and measurement

^{1}H NMR and FT-IR spectra

^{1}H NMR spectra were recorded on an Avancell 500 MHz spectrometer (Bruker, Switzerland) using $CDCl_3$ or DMSO-d_6 as the solvent and tetramethylsilane as the internal reference. FT-IR characterization was performed on a Nicolet Avatar 330 spectrophotometer (Thermo Electron Corporation, USA).

Gel permeation chromatography (GPC) measurement

The molecular weights of the oligomers and copolymers were determined by GPC (Waters, USA) using a Waters 1515 isocratic HPLC pump, coupled with a Waters 2414 refractive index detector and three Styragel columns (Waters HT4, HT5E and HT6). Tetrahydrofuran and polystyrene were used as the eluent and standard, respectively.

Atomic force microscopy (AFM)

The AFM images of the AEMs were recorded using an atomic force microscope (5500, Agilent Technologies) in a tapping mode under ambient condition. Before testing, the membrane samples were equilibrated at RT under a relative humidity (RH) of 60% for 24 h.

Small angle X-ray scattering (SAXS)

SAXS characterization was performed at RT under vacuum on a SAXSess-MC2 X-ray scattering spectrometer (Anton Paar, Austria). The scattering wave vector (q=4πsinθ/λ_i) ranges from 0.05 to 1.0 nm^{-1}, where θ and λ_i are the half of scattering angle and the incident wavelength, respectively.

Ionic exchange capacity (IEC)

The classical back-titration method was used to determine the IEC of the AEMs. Before testing, the OH^- form AEM sample was dried under vacuum at 60 °C for 48 h and immersed in a 0.1 M HCl solution for 24 h to ensure that all OH^- was fully ion-exchanged by Cl^-. The solution was then back titrated with a 0.05 M KOH solution. The IEC value (meq g^{-1}) is calculated from

$$IEC = \frac{M_{o,HCl} - M_{e,HCl}}{m_d} \times 100\% \quad (1)$$

where $M_{o,HCl}$ and $M_{e,HCl}$ (meq) are the milliequivalent of HCl before and after equilibrium, respectively, and m_d (g) is the weight of the dry membrane.

Water uptake (WU) and λ

The WU of the AEMs was measured via a quartz spring balance, as described in our previous publication.[29] The WU is calculated by Hooke's law

$$WU = \frac{kL_3 - kL_2}{kL_2 - kL_1} \times 100\% = \frac{L_3 - L_2}{L_2 - L_1} \times 100\% \quad (2)$$

where k is the elasticity coefficient of the quartz spring, L_1 is the initial length of the quartz spring, L_2 is the length of the quartz spring loaded with a dry AEM sample, and L_3 is the length of the quartz spring when the dry sample was swollen thoroughly. The average number of absorbed water molecules per ionic group, λ, is calculated from

$$\lambda = \frac{WU}{M_{H_2O}} \times \frac{1000}{IEC} \quad (3)$$

where M_{H2O} is the molecular weight of water (18.02 g mol^{-1}).

Swelling ratio (SR)

The SR of the membranes was determined by soaking a rectangular dry AEM sample in DI water at a given temperature. The dimensional change in the plane direction of the sample from the dry to wet state was measured. SR can be calculated by

$$SR = \frac{W_w \times L_w - W_d \times L_d}{W_d \times L_d} \times 100\% \quad (4)$$

where W_w and L_w are the width and length of the wet membrane, respectively, and W_d and L_d are the width and length of the dry membrane, respectively.

Ionic conductivity

The ionic conductivity (in-plane) of the AEMs was measured on a Parstat 263 electrochemical workstation (Princeton Advanced Technology, USA) by the two-electrode AC impedance spectroscopy method as reported previously.[14] Before the measurement, the membrane samples in OH^- form were soaked in DI water for at least 24 h. The testing was conducted at different temperatures from 30 to 80 °C by immersing the membrane samples in DI water in a chamber. During the testing, the chamber was charged with flowing N_2 gas to evacuate CO_2. The ionic conductivity (σ, S cm^{-1}) is calculated by

$$\sigma = \frac{l}{AR} \quad (5)$$

where R (Ω) is the resistance of the membrane, l (cm) is the distance between the two electrodes, and A (cm^2) is the cross-sectional area of the membrane.

Mechanical property

The mechanical properties of the AEMs were studied using a universal testing instrument (WDW-1E Testing System) at RT and 60% RH with a stretching speed of 10 mm min^{-1}. A 15 mm wide membrane sample was soaked in DI water at RT for 24 h before testing.

Thermal stability

The thermal stability of the membrane was characterized using a thermogravimetric analyzer (TGA, SDQT600, USA) at a heating rate of 10 °C min^{-1} from 30 to 750 °C in a nitrogen atmosphere. Before testing, the membrane was dried at 60 °C in a vacuum oven for 48 h.

Alkaline stability

To evaluate the alkaline stability of the membranes, the AEMs were soaked in a 2 M KOH solution at 60 °C for 600 h to investigate the change in chemical structure and ionic conductivity as a function of time. Before testing, the AEMs were washed repeatedly with DI water and soaked in DI water for more than 24 h.

Membrane electrode assembly (MEA) and single cell performance

MEA with the ImPPESN-2.87 and ImPESN-2.92 membranes was made by a method noted in the literature.[14,29] A catalyst-loaded carbon paper (1 mg cm^{-2} Pt, Johnson Matthey) treated by spraying with a homemade ionomer solution[29] was used as the anode/cathode electrodes and diffusion layer. The effective

electrode area was 4 cm^2. The MEA was fabricated by sandwiching the OH^- form AEM between the two electrodes and hot-pressed at 50 °C and 0.8 MPa for 10 min. The single cell test was carried out with H_2 (anode, 50 mL min^{-1}) and O_2 (cathode, 100 mL min^{-1}) at 60 ºC and 100% RH using an electronic load (ZY8714, ZHONGYING Electronic Co., Ltd.).

Results and Discussion

Synthesis and characterization of telechelic hydrophilic and hydrophobic oligomers

Three kinds of telechelic oligomers (oligomer-PF, oligomer-IF and oligomer-OH) were prepared via polycondensation as shown in Scheme 1. The chemical structure and oligomer lengths were characterized by ^{1}H NMR (Fig. S1†) and GPC (Table 1), respectively. Fig. S1(a)† shows the characteristic peaks of phenolphthalein groups clearly at 8.00, 7.78, and 7.63 ppm. Besides, protons on the terminal phenyl groups appeared for all of the as-synthesized telechelic oligomers, confirming the successful end-capping reaction. By adjusting the feed molar ratio of the hydroxyl-bearing monomer to the fluorine-bearing monomer, the degree of polycondensation was controlled at 22, 19 and 17 for oligomer-OH, oligomer-PF and oligomer-IF, respectively. All the results suggest the successful formation of the telechelic oligomers.

Synthesis and characterization of multiblock copolymers

Two kinds of multiblock copolymers (MPPESN and MPESN) with and without phenolphthalein groups on the hydrophilic segments were prepared by a copolymerization of oligomer-F (oligomer-PF or oligomer-IF) with oligomer-OH (Scheme 1). Fig. S2(a) and (b)† shows the ^{1}H NMR spectra of MPPESN and MPESN, respectively. The peaks around 2.05 ppm in both the two spectra are associated with protons of the benzylmethyl groups (a in Fig. S2†). A comparison with the ^{1}H NMR spectra of the starting oligomers (Fig. S1†) shows that all of the aromatic protons are well-assigned to the proposed multiblock copolymer structure, and the end-group peaks associated with the telechelic oligomers disappear. This indicates the successful formation of multiblock copolymers. Moreover, the copolymers have a sufficient large molecular weight (M_n>70 kDa, Table 1) for membrane formation.

Synthesis and characterization of brominated block copolymers

The synthesis of the BrPPESN-x and BrPESN-2.92 was performed in TCE using NBS as the brominating agent. Fig. S3(a) and (b)† shows the ^{1}H NMR spectra of BrPPESN-2.87 and BrPESN-2.92, respectively. A comparison of MPPESN (Fig. S2(a)†) and MPESN (Fig. S2(b)†) shows that new characteristic peaks corresponding to protons of the bromomethyl groups appeared at 4.17–4.33 ppm, and the peaks assignable to the benzylmethyl groups (a in Fig. S2†) decreased in size. Successful bromination of the benzylmethyl group on the multiblock copolymer is thus confirmed. The DF is calculated from ^{1}H NMR by DF = $12A_1/(3A_1+2A_2)$, where A_1 is the integrated area of the brominated benzyl peaks ($–CH_2Br$, two protons), and A_2 is the integrated area of the unreacted benzylmethyl peaks ($–CH_3$, three protons), as listed in Table 2. Furthermore, the BrPPESN-x with different DFs was prepared by varying the molar ratio of NBS to MPPESN, and the DF increased with increasing the molar ratio of NBS to MPPESN (Fig. S4†).

Table 1 Degree of polymerization (DP) and molecular weight of the oligomers and copolymers

Materials	DP Cal.[a]	DP Exp.[b]	M_n (Da)	M_w (Da)	M_w/M_n
oligomer-PF[29]	20	18.9	11136	17811	1.5994
oligomer-IF	20	17.2	8564	13392	1.5634
oligomer-OH[29]	20	21.9	7190	10583	1.4719
MPPESN[29]	--	--	71846	112185	1.6090
MPESN	--	--	76368	124822	1.6345

[a] The value calculated from the feed monomer ratio, [b] The value determined by GPC. All of the data of the oligomer-PF, oligomer-OH, MPPESN in this work were used with the permission from (COMPLETE REFERENCE CITATION), Copyright (2015), American Chemical Society.

Membrane formation and FI-IR spectra

As shown in Scheme 1, the ImPPESN-x and ImPESN-2.92 membranes were synthesized using 1-methylimidazole as the functional agent. Fig. S5(a) and (b)† shows the ^{1}H NMR spectra of the ImPPESN-2.87 and ImPESN-2.92 membranes, respectively. In both the spectra, the characteristic peaks at 9.13 ppm (H_1), 7.8–8.0 ppm (H_2 and H_3) and 3.6 ppm (H_4) are assigned to protons of the imidazolium ring, indicating the successful introduction of imidazolium cations. Furthermore, peaks at 4.17–4.33 ppm assigned to protons of $Ar–CH_2–Br$ disappeared almost completely and new peaks at 5.1–5.5 ppm assigned to protons of $Ar–CH_2–N$ appeared. This suggests the mostly conversion of $Ar–CH_2–Br$ to $Ar–CH_2–MIm$.

FT-IR spectra (Fig. S6†) further confirm the successful preparation of the Im-AEMs. The characteristic peaks at 2229 and 1244 cm^{-1} are attributed to the symmetric CN stretching vibration of nitrile groups and the asymmetric C–O stretching vibration of phenoxy groups, respectively.[30] The peaks at 1636 and 737 cm^{-1} are associated with the vibration of imidazolium cations, and the broad peak around 3404 cm^{-1} corresponds to the stretching vibration of –OH bonds. Both the ^{1}H NMR and FT-IR results confirm the structure of the ImPPESN-x and ImPESN-2.92 membranes.

Membrane morphology

Multiblock copolymers are well known to have an ability to form a hydrophilic/hydrophobic phase-separated morphology, which can provide continuous channels and thus facilitate ion transport. Fig. 1 shows the AFM images of the ImPPESN-2.87 and ImPESN-2.92 membranes. The dark and bright regions in the phase images are associated with the soft hydrophilic domains and the hard hydrophobic copolymer backbones, respectively. As can be seen, a well-defined phase-separated structure was formed in all of the two membranes. With a

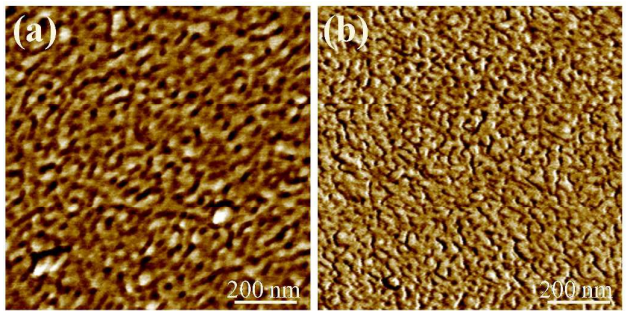

Fig. 1 AFM phase images of (a) ImPPESN-2.87[29] and (b) ImPESN-2.92. All the data of ImPPESN-2.87 in this work were used with the permission from (COMPLETE REFERENCE CITATION), Copyright (2015), American Chemical Society.

similar DF, ImPPESN-2.87 (Fig. 1(a)) had a much larger hydrophilic domain size and formed more developed interconnected ionic channels than ImPESN-2.92 (Fig. 1(b)). The chemical structure of the copolymer plays a critical role in phase separation and ionic aggregation. The hydrophilic domains of ImPPESN-2.87 are found to expand distinctly in size with the bulky phenolphthalein groups locating on the hydrophilic segments.

SAXS can be used to investigate the phase-separated structure and to quantify the ionic domain of the AEMs. As shown in Fig. 2, both the ImPPESN-2.87 and ImPESN-2.92 membranes displayed obvious peaks in the SAXS spectra. This suggests the formation of a microphase-separated structure between the hydrophilic and hydrophobic segments. The position of the ionomer peaks is found at q_{max}= 0.350 and 0.409 nm^{-1} for ImPPESN-2.87 and ImPESN-2.92, respectively. The corresponding interdomain spacing (d) of ImPPESN-2.87 and ImPESN-2.92 calculated from Bragg's law ($d=2\pi/q_{max}$) is 17.95 and 15.36 nm, respectively. The ionic domain spacing in ImPPESN-2.87 was larger than that in ImPESN-2.92, as confirmed by the AFM observation. This suggests that the presence of bulky phenolphthalein groups on the copolymer chains can expand the interchain spacing and increase ionic domain size. The larger ionic domains facilitate the formation of larger and more developed interconnected ion-transport channels. The hydrophilic/hydrophobic phase-separated structure is particularly important for AEMs. The effect of structure on the water absorption behavior and OH^- conductivity will be discussed below.

DF, IEC, water uptake (WU), λ, swelling ratio of the membranes

IEC represents the density of ion-exchangeable groups in the membranes. Table 2 shows that the IEC of the ImPPESN-x membranes is in the range of 0.81–2.48 meq g^{-1} from ^{1}H NMR and 0.75–2.36 meq g^{-1} from titration. The IEC increased with increasing the DF. This tendency is reasonable because larger DF means more bromomethyl groups on the BrPPESN chains, subsequently leading to larger number of imidazolium groups being grafted onto the membranes. The calculated and titrated IECs of ImPESN-2.92 are 2.22 and 2.10 meq g^{-1}, respectively. The titrated IEC of the as-prepared AEMs agreed well with that

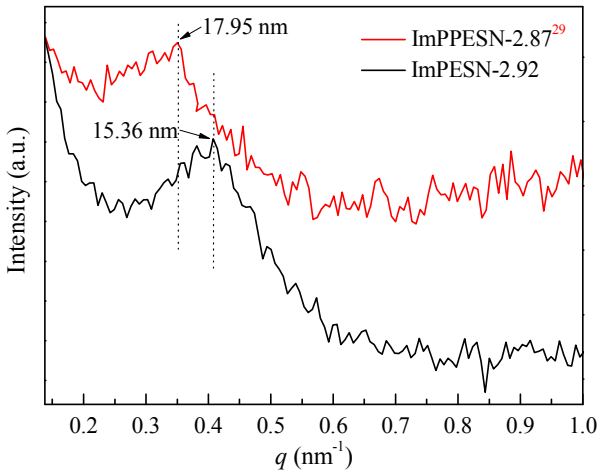

Fig. 2 SAXS patterns of the AEMs.

from ^{1}H NMR, demonstrating that Br^- was mostly replaced by OH^-.

Water uptake plays an important role in determining the ionic conductivity and mechanical properties of the AEMs. Water molecules within the AEMs can serve as the OH^- carrier and facilitate ion conducting. However, the AEMs cannot be used for practical applications if they swell too much in water. As listed in Table 2, both the water uptake and swelling ratio of the ImPPESN-x membranes increased with the temperature and the density of imidazolium groups. For comparison of the water uptake among various ImPPESN-x membranes, the number of absorbed water molecules per ionic group (designated as λ) was calculated. As shown in Table 2, with increasing the density of imidazolium groups, λ first increases and arrives at the maximum for ImPPESN-2.87. The reason is that increasing the density of the imidazolium groups in the ImPPESN membrane matrix would lead to an enhancement in the hydrophilicity of the membranes and thus the water absorption. Then λ declines from ImPPESN-2.87 to ImPPESN-3.36 with increasing the density of imidazolium groups. This is probable due to that the water absorption approaches the ultimate limit of the membrane material and constrains the increase of λ.

With a similar density of imidazolium groups, ImPPESN-2.87 (IEC=2.07 meq g^{-1}) displayed a much higher water uptake and λ, and a lower swelling ratio than ImPESN-2.92 (IEC=2.10 meq g^{-1}). The higher water uptake of ImPPESN-2.87 can be attributed to the formation of larger and more developed interconnected ionic channels for water molecules storage, as confirmed by AFM and SAXS. The lower swelling ratio suggests that the phenolphthalein groups suspended on the ImPPESN chain can suppress the swelling and enhance the dimensional stability effectively. As confirmed by SAXS, the introduction of bulky and rigid phenolphthalein groups in the copolymer chains can force each chain apart to expand the interchain spacing in which water molecules could be confined, resulting in lower swelling.[23,24]

Ionic conductivity

As a critical property of AEMs, the ionic conductivity of the

Table 2 DF, IEC, water uptake, λ, swelling ratio and mechanical properties of the AEMs [a]

Membrane	DF	IEC (meq g^{-1})		WU (%)		λ		SR (%)		Tensile strength	Elongation
		Cal.[b]	Exp.[c]	30 °C	60 °C	30 °C	60 °C	30 °C	60 °C	(MPa)	at break (%)
ImPPESN-0.94	0.94	0.81	0.75	10.1	13.2	7.4	9.8	5.7	7.6	45.3±0.4	23.8±0.4
ImPPESN-1.91	1.91	1.59	1.51	34.9	45.4	12.8	16.7	14.2	19.7	37.2±0.4	19.7±0.3
ImPPESN-2.87[29]	2.87	2.15	2.07	68.4	86.4	18.3	23.1	25.4	33.3	31.6±0.3	17.2±0.4
ImPPESN-3.36	3.36	2.48	2.36	76.8	95.8	18.0	22.5	31.9	44.5	23.6±0.3	12.5±0.2
ImPESN-2.92	2.92	2.22	2.10	56.4	70.0	14.9	18.5	32.4	47.1	27.1±0.2	14.3±0.3

[a] All of the data were obtained by averaging more than three experimental values, and the errors were less than 5%.[b] Calculated from the ^{1}H NMR spectra, [c] Estimated by back titration.

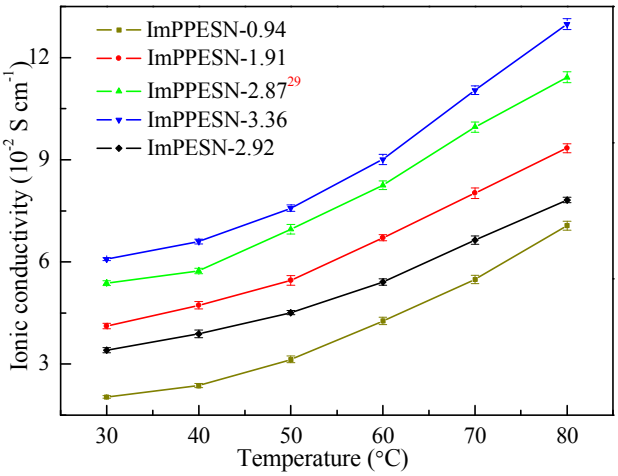

Fig. 3 Temperature dependence of the ionic conductivity of the AEMs.

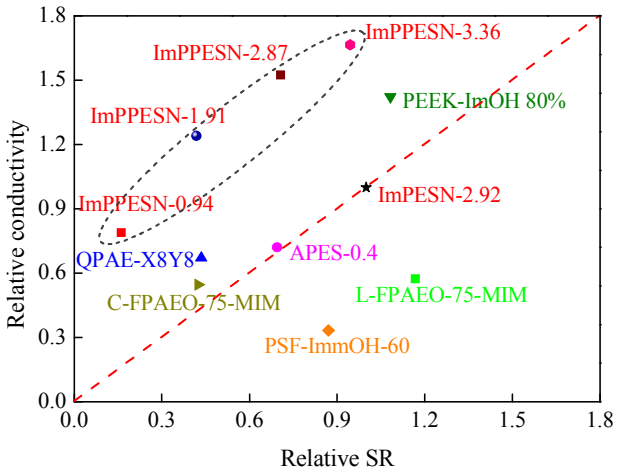

Fig. 4 Relative conductivity as a function of relative SR of the ImPPESN-x, ImPESN-2.92, PSf-ImmOH-60, C-FPAEO-75-MIM, L-FPAEO-75-MIM, QPAE-X8Y8, APES-0.4 and PEEK-ImOH 80% at 60 °C.

ImPPESN-x and ImPESN-2.92 membranes was measured in water at various temperatures. Fig. 3 shows that the ionic conductivity of the AEMs increased with increasing the temperature from 30 to 80 °C due to the improved water mobility. The ionic conductivity of the ImPPESN-x membranes also increased with increasing IEC and water uptake, and was in the range of 2.04−6.08×10^{-2} S cm^{-1} at 30 °C and 7.07−12.98×10^{-2} S cm^{-1} at 80 °C.

Similar to the water uptake, ImPPESN-2.87 exhibited a higher conductivity than ImPESN-2.92. As characterized by AFM and SAXS, ImPPESN-2.87 displayed a much clearer microphase-separated structure leading to larger and more developed interconnected ionic channels than ImPESN-2.92. As a result, ImPPESN-2.87 has a higher water uptake to facilitate OH^- transporting than ImPESN-2.92.

Furthermore, an important finding of this work is that the ImPPESN-x membranes showed much higher relative conductivity and lower relative swelling ratio than ImPESN-2.92. We used the ImPESN-2.92 membrane as the basis for comparison and set both the conductivity and swelling ratio of ImPESN-2.92 to be 1. The conductivity and swelling ratio of ImPPESN-x are divided by those of ImPESN-2.92 to get the relative conductivity and swelling ratio, respectively. As shown in Fig. 4, the ImPPESN-x membranes located on the top portion of the upper left-hand corner on the graph have larger relative conductivity and lower relative swelling ratio than ImPESN-2.92 and other AEMs with similar main chain structures (PSf-ImmOH-60 (random),[31] C-FPAEO-75-MIM (cross-linking),[32] L-FPAEO-75-MIM (random),[32] QPAE-X8Y8 (block),[33] APES-0.4 (block)[20] and PEEK-ImOH 80% (random)[34]). These results demonstrate that the present copolymer design of the ionic groups selectively and densely located on the phenolphthalein groups is effective at improving hydroxide conductivity and alleviating dimensional swelling for the AEMs.

Mechanical property

As another important character of the AEMs, the mechanical properties of the ImPPESN-x and ImPESN-2.92 membranes were evaluated at RT and 60% RH (Table 2). By increasing IEC, the tensile strength of ImPPESN-x decreased from 45.3±0.4 to 23.6±0.3 MPa, and the elongation at break decreased from 23.8±0.4% to 12.5±0.2%. As noted above,

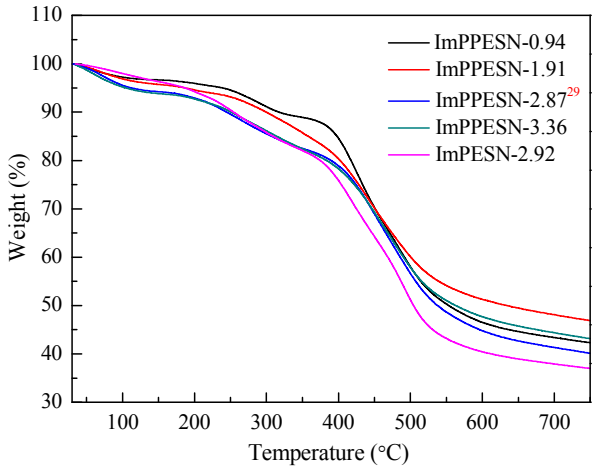

Fig. 5 TGA curves of the AEMs under a nitrogen atmosphere.

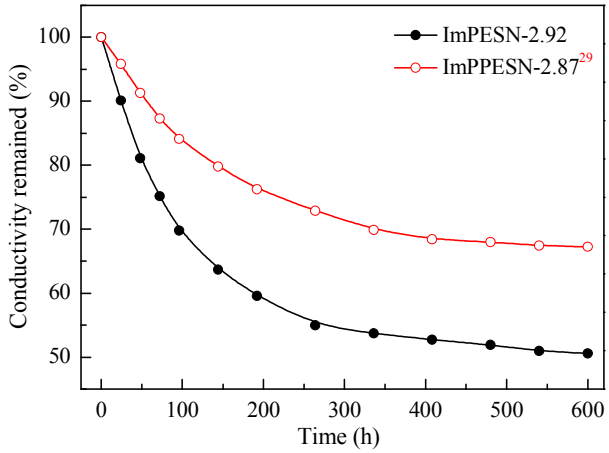

Fig. 6 Remaining conductivity of ImPPESN-2.87[29] and ImPESN-2.92 in a 2M KOH solution at 60 °C.

increasing IEC leads to an increase in the SR of the ImPESNC-x membranes subsequently degrades the mechanical properties due to the dimensional change in the AEMs. With a much lower swelling ratio, ImPPESN-2.87 showed a stronger tensile strength and a higher elongation at break than ImPESN-2.92.

Thermal stability

The thermal stability of the ImPPESN-x and ImPESN-2.92 membranes were investigated by TGA in a nitrogen atmosphere, as shown in Fig. 5. All the AEMs exhibited three distinct thermal degradation steps. Take ImPPESN-x as an example: (1) the initial slight weight loss from 30 to 150 °C was attributed to the evaporation of the residual solvent (DMSO) and absorbed water. (2) The second step in the range of 200–400 °C could be associated with the decomposition of the imidazolium groups, and the weight loss was approximately corresponding to the weights of the imidazolium groups in the membranes. (3) The third step above 400 °C was ascribed to the decomposition of the copolymer backbones. Especially, the maximum degradation rate of the backbone of ImPPESN-2.87 (at 446 °C) was at a higher temperature than that of ImPESN-2.92 (at 423 °C). This indicates that the introduction of phenolphthalein groups into the main chains could significantly improve the thermal stability.

Table 3 IEC and conductivity of ImPPESN-2.87[29] and ImPESN-2.92 before and after immersion in a 2M KOH solution at 60 °C for 600 h

	IEC[a] (meq g^{-1})		conductivity[b] (10^{-2} S cm^{-1})	
Membrane	before	after	before	after
ImPPESN-2.87[29]	2.07	1.61	5.38	3.62
ImPESN-2.92	2.10	1.18	3.41	1.74

[a] Estimated by back titration, [b] Measured at 30 °C.

Alkaline stability

The alkaline stability of ImPPESN-2.87 and ImPESN-2.92 was studied by soaking the membranes in a 2M KOH solution at 60 °C. The change in the ionic conductivity, IEC and chemical structure of the membranes was characterized. Fig. 6 shows a sharp decrease in ionic conductivity for both the membranes within 300 h, and then almost to be a constant afterward. As shown in Table 3, after testing for 600 h, about 67% (3.62×10^{-2} S cm^{-1}) and 51% (1.74×10^{-2} S cm^{-1}) ionic conductivity remained for ImPPESN-2.87 and ImPESN-2.92, respectively. After the alkaline stability test, the IEC of ImPPESN-2.87 and ImPESN-2.92 decreased from 2.07 to 1.61 meq g^{-1} and from 2.10 to 1.18 meq g^{-1}, respectively.

The chemical structure of the membranes was characterized via FT-IR and ^{1}H NMR after the alkaline stability test. The peak at 2229 cm^{-1} (Fig. S6†) assigned to the nitrile groups without a significant change indicates the integrity of the nitrile groups. As shown in Figs. S7 and S8†, a clear decrease in the intensity of the peaks (9.13, 8.0, 7.8, 5.3, 3.6 ppm) associated with the imidazolium group is observed after the alkaline stability test. ImPESN-2.92 has a higher degradation degree than ImPPESN-2.87. This suggests a more serious degradation of the imidazolium group in ImPESN-2.92 than in ImPPESN-2.87.

This observation reveals ImPPESN-2.87 exhibiting a better alkaline stability than ImPESN-2.92. First, the stability of imidazolium groups is assumed to be enhanced by the presence of the bulky cardo groups because they provide high steric effects and hinder the attack by hydroxyl ions. A similar behavior was also noted for the fluorine-containing AEMs.[14] Second, the difference in the hydrophilic/hydrophobic microphase-separated morphology between the two membranes could also play an important role. According to Pratt's[35] and Pivovar's[36] calculation, a better solvation of OH^- in the AEMs would lead to a slower degradation of the cation. As shown in AFM and SAXS, ImPPESN-2.87 has a much larger hydrophilic domain size and more developed interconnected ionic channels than ImPESN-2.92. Most of the imidazolium groups and counter ions (OH^-) are thought to be 'bathed' in those channels. ImPPESN-2.87 can thus provide a better solvation environment

for OH^- subsequently result in a higher alkaline stability of the imidazolium groups in it.[37,38]

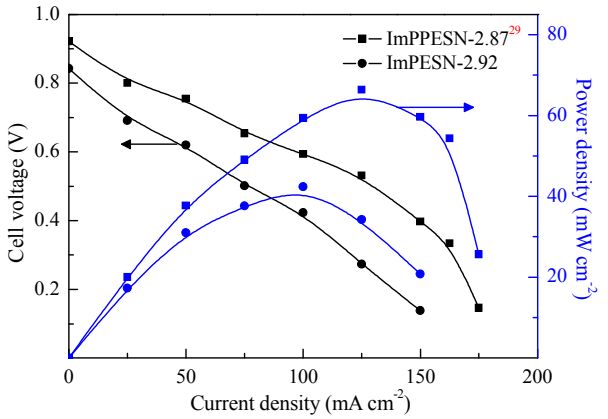

Fig. 7 Performances of a single cell using ImPPESN-2.87[29] and/or ImPESN-2.92 at 60 °C (100% RH).

Single cell performance

Fig. 7 shows the performance of a single cell (H_2/O_2) using ImPPESN-2.87 and/or ImPESN-2.92 with a thickness of 39 μm at 60 ºC and 100% RH. ImPPESN-2.87 exhibits a higher open circuit voltage (0.92 V) and a higher maximum power density (66.4 mW cm^{-2}) than ImPESN-2.92 (0.84 V and 42.3 mW cm^{-2}). The better performance in single cell evaluation may be due to the lower swelling ratio and higher conductivity of ImPPESN-2.87 at 60 ºC.[39] Furthermore, other properties including the comparability of the membrane with the ionomer, water uptake, mechanical properties, thermal and alkaline stability are also critical for the final electrochemical property.[39] Besides the AEMs' properties, the single cell behavior is also affected by many other factors such as catalyst loading, operating condition and the MEA fabrication procedures.[40,41]

Conclusions

Two kinds of multiblock PESN AEMs, in which the ion groups were selectively and densely located on the phenolphthalein-sulfone segments for one and the bisphenol A-sulfone segments for the other, were synthesized by block copolycondensation, bromination, imidazolium-functionalization and hydroxide ion exchange. The membrane morphology structure analyses suggested that the presence of bulky phenolphthalein groups on the hydrophilic segment of multiblock copolymer could expand the interchain spacing and ionic domain size and facilitate the formation of larger and more developed interconnected ion-transport channels in the membranes. The water uptake, swelling ratio, hydroxide conductivity of the ImPPESN-x membranes increased with increasing the IEC. With a similar IEC, ImPPESN-2.87 showed lower swelling ratio, higher water uptake and mechanical properties, much higher hydroxide conductivity, and better thermal and alkaline stability than ImPESN-2.92. These results indicated that the introduction of phenolphthalein groups into the hydrophilic segments of multiblock copolymer is effective at improving the ionic conductivity and alkaline stability of AEMs. The single cell test shows that the ImPPESN-2.87 membrane exhibits a more excellent H_2/O_2 fuel cell performance. This suggests that the ImPPESN membranes are promising for alkaline fuel cells.

Acknowledgment

Financial support from the National Nature Science Foundation of China (grant nos. 21376194 & 21576226), the Nature Science Foundation of Fujian Province of China (grant no. 2014H0043), and the research fund for the Priority Areas of Development in Doctoral Program of Higher Education (no. 20130121130006) is gratefully acknowledged. We are very thankful for the referees' helpful comments.

Notes and references

1 H. Zhang and P. K. Shen, *Chem. Rev.*, 2012, **112**, 2780–2832.
2 M. A. Hickner, *Mater. Today*, 2010, **13**, 34–41.
3 B. Dong, L. Gwee, D. S. Cruz, K. I. Winey and Y. A. Elabd, *Nano Lett.*, 2010, **10**, 3785–3790.
4 R. Akiyama, D. Hirayama, M. Saito, J. Miyake, M. Watanabe and K. Miyatake, *RSC Adv.*, 2013, **3**, 20202–20208.
5 R. Borup, J. Meyers, B. Pivovar, Y. S. Kim, R. Mukundan, N. Garland, D. Myers, M. Wilson, F. Garzon, D. Wood, P. Zelenay, K. More, K. Stroh, T. Zawodzinski, J. Boncella, J. E. McGrath, M. Inaba, K. Miyatake, M. Hori, K. Ota, Z. Ogumi, S. Miyata, A. Nishikata, Z. Siroma, Y. Uchimoto, K. Yasuda, K. Kimijima and N. Iwashita, *Chem. Rev.*, 2007, **107**, 3904–3951.
6 J. R. Varcoe, P. Atanassov, D. R. Dekel, A. M. Herring, M. A. Hickner, P. A. Kohl, A. R. Kucernak, W. E. Mustain, K. Nijmeijer, K. Scott, T. Xu and L. Zhuang, *Energy Environ. Sci.*, 2014, **7**, 3135–3191.
7 G. Merle, M. Wessling and K. Nijmeijer, *J. Membr. Sci.*, 2011, **377**, 1–35.
8 W. Sheng, A. P. Bivens, M. Myint, Z. Zhuang, R. V. Forest, Q. Fang, J. G. Chen and Y. Yan, *Energy Environ. Sci.*, 2014, **7**, 1719–1724.
9 O. Kim, G. Jo, Y. J. Park, S. Kim and M. J. Park, J. Phys. *Chem. Lett.*, 2013, **4**, 2111–2117.
10 N. Li and M. D. Guiver, *Macromolecules*, 2014, **47**, 2175–2198.
11 C. H. Park, C. H. Lee, J. Y. Sohn, H. B. Park, M. D. Guiver and Y. M. Lee, *J. Phys. Chem. B*, 2010, **114**, 12036–12045.
12 Y. A. Elabd and M. A. Hickner, *Macromolecules*, 2011, **44**, 1–11.
13 A. H. N. Rao, S. Y. Nam and T. H. Kim, *J. Mater. Chem. A*, 2015, **3**, 8571–8580.
14 P. Y. Xu, K. Zhou, G. L. Han, Q. G. Zhang, A. M. Zhu and Q. L. Liu, *ACS Appl. Mater. Interfaces*, 2014, **6**, 6776–6785.
15 A. K. Singh, R. P. Pandey and V. K. Shahi, *RSC Adv.*, 2014, **4**, 22186–22193.
16 W. H. Lee, A. D. Mohanty and C. Bae, *ACS Macro Lett.*, 2015, **4**, 453–457.
17 M. Zhang, J. Liu, Y. Wang, L. An, M. D. Guiver and N. Li, *J. Mater. Chem. A*, 2015, **3**, 12284–12296.
18 X. Li, G. Nie, J. Tao, W. Wu, L. Wang and S. Liao, *ACS Appl. Mater. Interfaces*, 2014, **6**, 7585–7595.
19 M. A. Hossain, Y. Lim, S. Lee, H. Jang, S. Choi, Y. Jeon, J. Lim and W. G. Kim, *Int. J. Hydrogen Energy*, 2014, **39**, 2731–2739.

20 P. Y. Xu, K. Zhou, G. L. Han, Q. G. Zhang, A. M. Zhu and Q. L. Liu, *J. Membr. Sci.*, 2014, **457**, 29–38.
21 E. A. Weiber and P. Jannasch, *J. Membr. Sci.*, 2015, **481**, 164–171.
22 H. Jang, M. M. Islam, Y. Lim, S. Lee, M. A. Hossain, T. Hong, S. Lee, Y. Hong and W. G. Kim, *Solid State Ionics*, 2014, **262**, 845–851.
23 J. Zheng, J. Wang, S. Zhang, T. Yuan and H. Yang, *J. Power Sources*, 2014, **245**, 1005–1013.
24 J. Zheng, Q. He, N. Gao, T. Yuan, S. Zhang and H. Yang, *J. Power Sources*, 2014, **261**, 38–45.
25 N. Gao, F. Zhang, S. Zhang and J. Liu, *J. Membr. Sci.*, 2011, **372**, 49–56.
26 S. Yun, J. Parrondo and V. Ramani, *J. Mater. Chem. A*, 2014, **2**, 6605–6615.
27 Y. Xiong, Q. L. Liu and Q. H. Zeng, *J. Power Sources*, 2009, **193**, 541–546.
28 L. Li and Y. Wang, *J. Membr. Sci.*, 2005, **262**, 1–4.
29 A. N. Lai, L. S. Wang, C. X. Lin, Y. Z. Zhuo, Q. G. Zhang, A. M. Zhu and Q. L. Liu, *ACS Appl. Mater. Interfaces*, 2015, **7**, 8284–8292.
30 Q. Zhang, B. Liu, W. Hu, W. Xu, Z. Jiang, W. Xing and M. D. Guiver, *J. Membr. Sci.*, 2013, **428**, 629–638.
31 Y. Yang, J. Wang, J. Zheng, S. Li and S. Zhang, *J. Membr. Sci.*, 2014, **467**, 48–55.
32 W. Wang, S. Wang, W. Li, X. Xie and Y. lv, *Int. J. Hydrogen Energy*, 2013, **38**, 11045–11052.
33 X. Li, Y. Yu, Q. Liu and Y. Meng, *J. Membr. Sci.*, 2013, **436**, 202–212.
34 X. Yan, S. Gu, G. He, X. Wu and J. Benziger, *J. Power Sources*, 2014, **250**, 90–97.
35 S. Chempath, B. R. Einsla, L. R. Pratt, C. S. Macomber, J. M. Boncella, J. A. Rau and B. S. Pivovar, *J. Phys. Chem. C*, 2008, **112**, 3179–3182.
36 S. Chempath, J. M. Boncella, L. R. Pratt, N. Henson and B. S. Pivovar, *J. Phys. Chem. C*, 2010, **114**, 11977–11983.
37 K. W. Han, K. H. Ko, K. Abu-Hakmeh, C. Bae, Y. J. Sohn and S. S. Jang, *J. Phys. Chem. C*, 2014, **118**, 12577–12587.
38 Z. Zhang, L. Wu, J. Varcoe, C. Li, A. L. Ong, S. Poynton and T. Xu, *J. Mater. Chem. A*, 2013, **1**, 2595–2601.
39 Y. Zhao, H. Yu, F. Xie, Y. Liu, Z. Shao and B. Yi, *J. Power Sources*, 2014, **269**, 1–6.
40 N. Li, Y. Leng, M. A. Hickner and C. Y. Wang, *J. Am. Chem. Soc.*, 2013, **135**, 10124–10133.
41 L. Zeng, T. S. Zhao and L. An, *J. Mater. Chem. A*, 2015, **3**, 1410–1416.